Granular Matter
DOI 10.1007/s10035-011-0250-y

ORIGINAL PAPER

Percolating contact subnetworks on the edge of isostaticity

David M. Walker · Antoinette Tordesillas · Colin Thornton · Robert P. Behringer · Jie Zhang · John F. Peters

Received: 18 September 2010
© Springer-Verlag 2011

Abstract We search for a percolating, strong subnetwork of contacts in a quasi-statically deforming, frictional granular material. Of specific interest in this study is that subnetwork which contributes to the majority of the total deviator stress and is, or is on the edge of being, isostatic. We argue that a subnetwork derived from the minimal spanning trees of a graph—optimized to include as many elastic contacts as possible and which bear normal contact forces above a given threshold delivers such a network. Moreover adding the strong 3-force-cycles to the spanning tree introduces a level of redundancy required to achieve a network that is almost if not isostatic. Results are shown for assemblies of non-uniformly sized circular particles under biaxial compression, in two-dimensions: a discrete element (DEM) simulation of monotonic loading under constant confining pressure, and cyclic loading of photoelastic disks under constant volume.

D. M. Walker · A. Tordesillas (✉)
Department of Mathematics and Statistics, University of Melbourne, Parkville, VIC 3010, Australia
e-mail: atordesi@ms.unimelb.edu.au

C. Thornton
School of Chemical Engineering, University of Birmingham, Birmingham, B15 2TT, UK

R. P. Behringer
Department of Physics, Duke University, Box 90305, Durham, NC 27708, USA

J. Zhang
CNLS/MPA-CMMS, Los Alamos National Lab, Los Alamos, NM 87545, USA

J. F. Peters
US Army Engineer Research & Development Center, Vicksburg, MS 39180-6199, USA

Keywords Complex networks · Spanning trees · Force chains · Force cycles · Isostatic

1 Introduction

Ioannis Vardoulakis and his collaborators brought soil mechanics to a level comparable to other disciplines of continuum mechanics and as a result enriched both. His studies of shear bands (strain localization), Cosserat theory, and stability brought those subjects into the mainstream at a time when the numerical analysis community was struggling with the validity of constitutive theories for frictional media *viz. a viz.* the mathematical well-posedness of associated initial and boundary value problems. The intense interest seen today in micropolar theory is a direct result of his work. AT's last face-to-face conversation with Ioannis was on micropolar constitutive models that explicitly accounted for force chain evolution [1]. In this discussion, Ioannis raised a model that he developed in the late 80s in which he envisaged the granular medium to be a 'two-fractions mixture'—comprising 'weak or frail' and 'strong or competent' grains [2]. This study was inspired by that paper. Using a complex networks approach, we explore other properties exhibited by these two fractions in connection with the macroscopic stress and the structural mechanics concept of redundancy. As this study integrates several key concepts and developments in the physics and mechanics of granular systems, we provide first an exposition of these to put into context this effort before presenting our findings.

Features that have both orientation and spatial extent, exemplified by the so-called force chains (the strong grains in [2]), dominate the micromechanics of granular media yet fall outside the domain of traditional 'local' continuum mechanics. In devising alternative continuum theories based

uncorrected proof

Journal: 10035 Article No.: 0250 MS Code: GRMA-D-10-00058.2 ☐ TYPESET ☐ DISK ☐ LE ☐ CP Disp.:2011/1/20 Pages: 7 Layout: Large

on non-local and micropolar formalisms one must reckon with the general lack of empirical evidence to account for structural evolution, boundary conditions and geometric configuration of the material domain. Data extracted from discrete element method (DEM) simulations and photoelastic disk experiments [3–8], provide a wealth of information to support non-traditional theories. Details on force chain evolution form a key outcome that has profound implications for the broad science of granular materials and especially for constitutive theory.

One of us, CT, notes that in the 90s there was much interest in 'strong force chains' of particles and their contribution to the macroscopic stress that quantifies the load-bearing capacity of the material. However, the stress tensor is a function of the contact information, forces and local coordinates, rather than the particles themselves. In this context, Radjai et al. [9] showed that, for 2D systems of rigid disks, the deviatoric stress was entirely due to the strong subnetwork of contacts transmitting larger than average contact forces. This was confirmed in [10] from 3D DEM simulations of 'soft' spheres, irrespective of the elastic properties of the particles. Thornton [11] also showed that the tangential contact forces only provided a small (typically $\sim$ 15%) contribution to the deviator stress. The same was found in triaxial compression tests for various granular assemblies comprising irregularly-shaped particles [12]. Moreover, for general states of stress ($\sigma_1 \neq \sigma_2 \neq \sigma_3$), it was demonstrated in [13] that any deviation from the isotropic stress state, i.e. the deviatoric stress, was almost entirely due to the strong subnetwork of contacts each transmitting larger than the global average force. A review of studies focussed on exploring the connection between the strong subnetwork of contacts and the macroscopic stress for various loading conditions is given in [14]. Overall, these observations suggest the possibility that the strong contact network, described by Radjai and co-workers as the "solid-like backbone" of the material [9]—may be isostatic but is embedded within the overall redundantly constrained (hyperstatic or statically indeterminate) particle system. Indeed man-made structures depend crucially on redundant supports to maintain stability [15].

While the force chain network by themselves might be close to if not isostatic, structural mechanics dictates that contacts from laterally confining neighbors are needed to provide these columnar load-bearing force chains with the necessary redundancies to maintain stability. In past analyses of 2D and 3D systems, columnar force chains have been found to consistently reside in self-organized local contact topologies with a relatively higher level of connectivity [6–8]. This is evident in force chain particles having a higher average number of contacts as well as stabilizing 3-cycles (i.e. contacts with neighbors which are themselves in mutual contact) when compared to other particles in the system. The process of self-organization in these dense granular systems seems to follow 'rules' resembling those employed in the construction of man-made structures. Specifically, the system in the stable regime (e.g. during strain-hardening in the biaxial tests in [6]) evolves to form a macroscopically redundant structure comprising, at the mesoscopic scale, axial load bearing column-like force chains which are laterally supported by truss-like 3-cyles. However, as shown in [6], the bulk redundancy of the system degrades with dilatation, following the loss of contacts in the direction of extension, with the greatest rate of decrease in the average number of contacts per particle recorded during the unstable strain-softening regime. Evidence that redundancy aids material stability can be seen during the initial force chain buckling event: although this may involve the collapse of multiple force chains, this critical event occurs just prior to peak shear stress when the material is globally stable [6]. That the material holds post-critical strength or load-carrying capacity amidst collapse of some of its major load bearing members—is due to its capability to redistribute its internal forces and moments to other contacts. This is often seen in engineering structures which are commonly endowed with sufficient redundancies for stability and safety as highlighted in [15]: *"For example, when a single column of a large frame buckles, the entire frame need not collapse, since the axial force from this column can be transferred to the adjacent columns."*

In experiments and other DEM simulations, isostatic, hyperstatic and hypostatic regimes have been observed to co-exist simultaneously in different spatial regions [7]. Specifically, in experiments on photoelastic disks subjected to multiple cycles of pure quasi-static shear at constant volume [5,7], shearbands form, and force chains develop, strengthen and buckle, all accompanied by fluctuations of local packing densities. During the start of this process, the system evolves from a stress-free initial state to an intermediate hypostatic regime below jamming, then to an isostatic regime near jamming, and finally arrives at a hyperstatic state. Under shear reversal after reaching some maximum strain, force networks change adaptively to the switch in the shear direction: the original force network melts away, in part through loss of contacts in the direction perpendicular to the applied compression, and a new force network forms with force chains aligned along the direction of the applied compression.

The nature of jamming has been the focus of several recent reviews [16–18] with the key concepts revolving around states which can be described as hypostatic, isostatic, or hyperstatic. Here, the number of contacts per particle (denoted typically by Z), plays an important role in distinguishing stability. States with too few contacts, such that there are so-called floppy modes which allow deformation within the system without energy cost, are hypostatic. States where there are no such floppy modes are hyperstatic, and isostaticity separates hyperstatic and hypostatic states.

Uncorrected Proof

Journal: 10035 Article No.: 0250 MS Code: GRMA-D-10-00058.2 ☐ TYPESET ☐ DISK ☐ LE ☐ CP Disp.:2011/1/20 Pages: 7 Layout: Large

Granular materials near isostatic states can show critical-like behavior in terms of the particle rearrangement to external perturbations [19], divergence of a characteristic length scale to a point force response [20,21], an enhancement of the number of normal modes at zero frequency [22], and anomalous behaviors near the special jamming transition point, J [17,23]. By applying coarse graining, Blumenfeld has been able to demonstrate that in isostatic systems, the governing system of equations on large scales may be hyperbolic: this leads to a natural association between force chains and the characteristics of the system of equations for such media [24,25]. In the same paper [24], Blumenfeld also proposed that systems which are close to but not identically isostatic, may be treated as a mixture of two phases with one phase being isostatic and the other consisting of a connected, hyperstatic, regime. However, it is not clear how those two phases should be identified in different spatial regions.

In this study, we explore the extent to which a percolating strong subnetwork of contacts satisfies the isostatic condition in a DEM simulation of monotonic biaxial loading and in an experimental cyclic shear test. Previous studies have assumed a contact force threshold $f_c = F/\langle F\rangle = 1$ to identify the 'strong' network, where $\langle F\rangle$ is the global average force. Here we relax this constraint and, in addition, search for an isostatic percolating subnetwork that maximizes the contribution to the deviator stress. The algorithm we propose allows us to separate the contact networks into two parts—a strong network and a weak supporting network. To do so, we use two methods: one based on the value of R defined in (2) of Methods (and elsewhere [7]) and the other using the average force as the threshold. The former produces a subnetwork which is exactly at the isostatic state at $R = 1$. However, we emphasize here that our method is general; it can be applied to any hyperstatic system, whether the system itself is near isostatic state or far from the isostatic state.

2 Methods

An assembly of granular particles can be represented by a mathematical graph or complex network, where the network nodes correspond to particles and the links to contacts. The rheological response of the material to loading is encoded in evolving properties of this contact network [26]. The *strong (weak) contacts* of a network are those contacts which carry a normal contact force magnitude above (below) a given threshold, where traditionally, the dividing point between strong and weak is taken to be the global mean, or in normalized form, $f_c = 1$. The *stress* is given (here for circular particles) by

$$\hat{\sigma}_{ij} = \frac{1}{\sum_{p\in N_p} V^p} \sum_{c\in N_c^L} n_i^{Ac} f_j^{Ac} (R^{Ac} + R^{Bc}) \qquad (1)$$

where N_p is the set of particles in the network, V^p is the local void volume of a particle, N_c^L represents the number of contacts in the subnetwork L, f_j^{Ac} is the contact force between particle A and particle B, n_i^{Ac} is the unit branch vector of the contact and R^{Ac} and R^{Bc} are the radii of the contacting particles. Equation (1) gives the stress for the solid phase of the assembly rather than the whole volume, the two differing by a multiplicative factor equal to the solids fraction. The percolating subnetwork shares the same physical space as the whole assembly, thus for purposes of comparison, we simplify our computation by using solid fraction stresses. The deviator stress (i.e. second invariant of the deviatoric stress tensor) is thus given by the difference in the eigenvalues of the stress tensor, i.e. $D = \frac{1}{2}[\max(\lambda_i) - \min(\lambda_i)]$, where λ_i are the eigenvalues of $\hat{\sigma}_{ij}$.

An assembly of grains in equilibrium is *isostatic* if there is exactly enough contacts for force and torque, or moment, balance: i.e. the number of unknown independent forces and moments is equal to the number of equilibrium equations. If the assembly is under-constrained (over-constrained), i.e. the number of unknown independent forces and moments is less (greater) than the number of equilibrium equations, then the network is *hypostatic* (*hyperstatic*). The redundancy of a granular assembly can be quantified using a procedure discussed in detail in [7] but key elements are repeated here for the benefit of the reader. A scalar ratio R can be defined where $R < 1$ corresponds to a hypostatic system, $R = 1$ to an isostatic system, and $R > 1$ indicates a hyperstatic system. The definition of R accounts for the number and types/modes of contact in a network. The contacts are classified according to whether they are elastic or plastic with a further distinction accounting for rolling resistance (contact moment) in assemblies of circular disks. In particular, a *stick* contact is such that both the tangential force and contact moment are elastic and independent of the normal force; by contrast, a *sliding* contact is such that the tangential force is at the Coulomb threshold and thus coupled to the normal force and a *rolling* contact is such that the contact moment is at its analogous Coulomb plastic threshold and thus also coupled to the normal force. A *sliding and rolling* contact has both tangential force and contact moment at their respective Coulomb plastic thresholds. Specifically, in 2D R, the ratio of the number of independent forces *and* moments to the number of equilibrium equations, is given by

$$R = \frac{3N_{\text{stick}} + 2N_{\text{slide}} + 2N_{\text{roll}} + N_{\text{slide+roll}}}{3N_{\text{particles}}}, \qquad (2)$$

where N_{stick}, N_{slide}, N_{roll} and $N_{\text{slide+roll}}$ are the number of stick, sliding, rolling, and sliding+rolling contacts in the subnetwork. $N_{\text{particles}}$ is the number of particles in the subnetwork. The pre-factors in (2) represent the number of degrees of freedom needed to define each type of contact. For example, a stick contact is below the limiting state for all modes

Uncorrected Proof

Journal: 10035 Article No.: 0250 MS Code: GRMA-D-10-00058.2 TYPESET DISK LE CP Disp.:2011/1/20 Pages: 7 Layout: Large

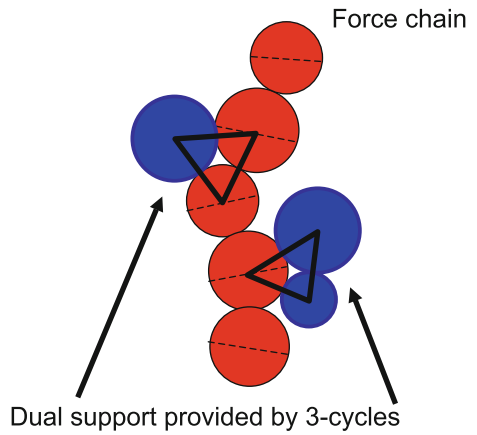

Fig. 1 An example of the dual supporting role to force chains that 3-cycles provide (i.e. resistance to relative rotations at contact and lateral support to 'prop-up' force chains). If the normal contact force carried at each edge of the *triangle* is above average (or a prescribed force threshold) then the cycle is a 3-force-cycle. If both 3-cycles above are 3-force-cycles then the union of contacts in each cycle constitutes the 3-force-cycle network

of deformation which requires three degrees of freedom in 2D. In contrast if the contact is sliding (rolling), a degree of freedom is removed because the tangential component of the contact force (contact moment) is coupled to the normal force, thus the multiple is two [7].

A subnetwork *percolates* the material domain if its constituent set of contacts extend from one boundary of the domain to the other. A *spanning tree* of a contact network is an acyclic subset of contacts that connects all the nodes. A minimal spanning tree is a spanning tree with minimum total path length or contacts. If we assign a weight to each contact or link, it is a spanning tree with minimum sum of contact weights. We weight the contact matrix according to contact mode: 1 for a stick contact, 2 for a rolling contact, 3 for a sliding contact, and 4 for the sliding+rolling contacts. Thus we bias the search for a minimal spanning tree towards finding stick and rolling contacts—the typical contact modes within the force chain network [1,27].

The 3-*force-cycles* within a network are the 'strong' 3-cycle motifs: the force (or, here, its normal component) at each contact of a 3-force-cycle has a magnitude that is at least the prescribed threshold. In [6] the 3-force cycles were introduced and discovered to play an important supporting role to force chains during and in the location of shear banding. As illustrated in Fig. 1, the 3-force cycles provide dual resistance to force chain buckling by: (1) frustrating particle rotations crucial for buckling and (2) propping-up the force chain particles. The 3-force-cycle network is the collection of all such 3-cycles (see, the red triangle contacts within the subnetworks of Fig. 2 for examples of such networks).

Our algorithm for finding a percolating and isostatic subnetwork proceeds in the following sequence:

1. Set the normal contact force magnitude threshold (e.g. $f_c = 1$).
2. Prune all contacts bearing a normal force magnitude less than f_c.
3. From the remaining contact subnetworks of step 2
   (a) Find the 3-force-cycle network.
   (b) Find the minimal spanning trees with the contacts weighted by contact type.
   (c) Construct the subnetwork comprising the union of contacts in the 3-force-cycle network and all the minimal spanning trees
4. If we require a force threshold such that the subnetwork is isostatic, i.e. $R = 1$, update the force threshold and return to step 2. The threshold can be updated using the Nelder-Mead simplex method to minimize the cost function $(R - 1)^2$.

For the resulting subnetwork of contacts, we compute the redundancy and its contribution to the total deviator stress. *Almost all* of the force chain particles, as determined from the algorithm used in [28], will be nodes for a force threshold of $f_c = 1$ or less. Note that some particles may be missed as the force chain algorithm of [28] considers only particles with above-average particle load vector magnitude and not above-average normal contact force. That is, the algorithm to find force chains within a granular assembly in equilibrium identifies groups of three or more contacting particles whose particle load vectors are: (1) in quasi-linear arrangement (i.e. consecutive vectors align to within a prescribed tolerance angle), and (2) each with a magnitude that is above the global average (see [28] for full details).

It is very difficult to find a force threshold such that the collection of minimal spanning trees is isostatic. The redundancy R from (2) for $f_c = 1$ and almost all other values above $f_c = 1$ are below 1.0. We must therefore add some contacts to the spanning trees to increase the redundancy. Recent studies of the topology of laterally supporting contacts around force chains from DEM simulations and physical experiment show, on average, that force chains not only have a higher number of contacts but also a higher number of 3-cycles per particle [6,7]. Accordingly, we consider the union of the spanning trees and the subnetwork of 3-force-cycles, the strong 3-cycles, for the given threshold.

3 Results

We present results of applying the above algorithm to two data sets, both 2D systems of polydisperse frictional circular particles, discussed extensively elsewhere. The first is from a DEM simulation of biaxial compression with constant confining pressure [1,6,7,26]. The second is from experiments

Uncorrected Proof

Journal: 10035 Article No.: 0250 MS Code: GRMA-D-10-00058.2 ☐ TYPESET ☐ DISK ☐ LE ☐ CP Disp.:2011/1/20 Pages: 7 Layout: Large

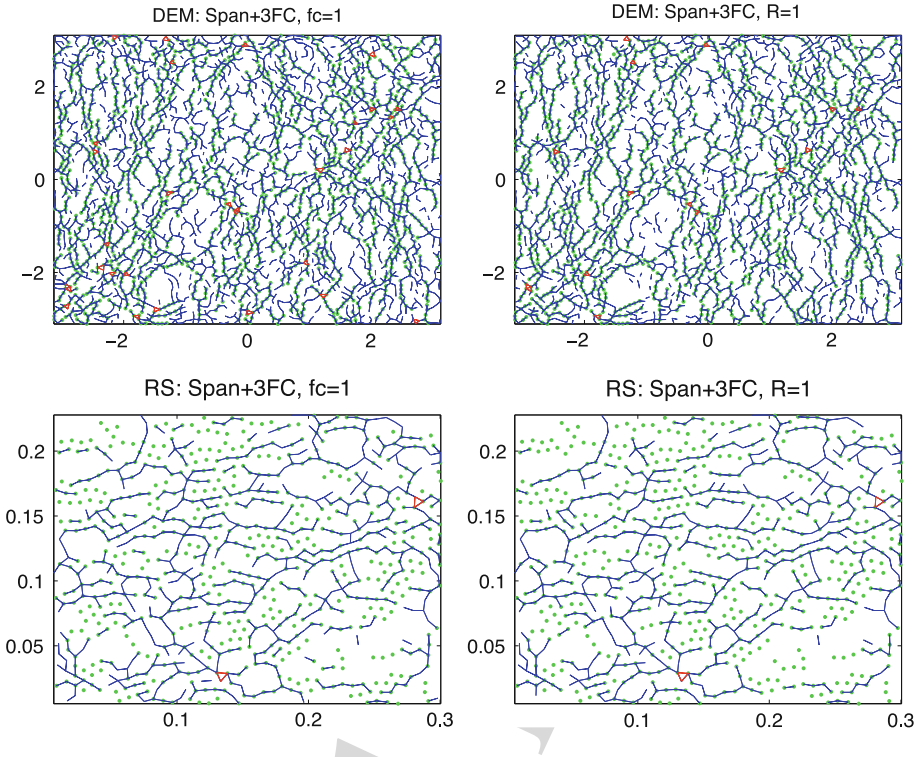

Fig. 2 Color online. Snapshots of the percolating minimal spanning trees and 3-force-cycle subnetworks (Span+3FC) for DEM at axial strain 0.04 (*upper*) and for cyclic shear system at strain step 417 (*lower*). Contacts are *blue*, 3-force-cycles contacts are *red triangles* and force chain nodes are *green*

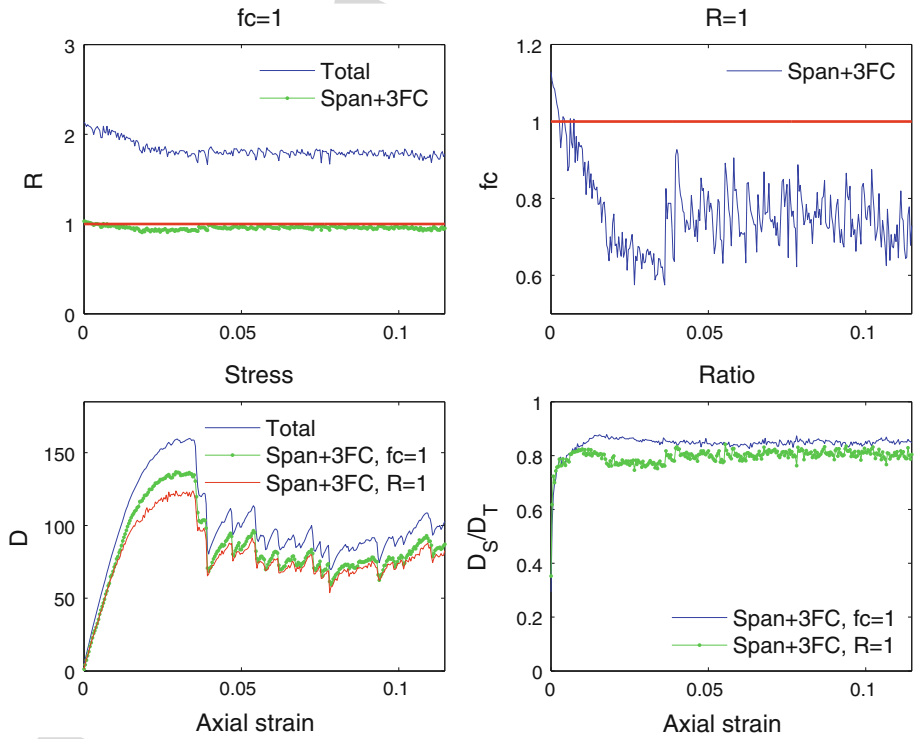

Fig. 3 Color online. DEM system—*Top left*: The redundancy of the networks at $f_c = 1$. *Top right*: the force threshold required such that the subnetwork (Span+3FC) is isostatic. *Bottom left*: the deviator stress $f_c = 1$ and $R = 1$. *Bottom right*: contribution to deviator stress of the subnetworks

using photoelastic disks subject to cyclic shear under constant volume [5,7]. Figure 2 (top row) shows the percolating subnetworks, i.e. union of minimal spanning trees and 3-force-cycles, for $f_c = 1$ and $R = 1$ in the DEM; the bottom row is for one strain step of the cyclic shear experiment. Quantities of interest for the subnetworks in the DEM simulation are shown in Fig. 3. We see for $f_c = 1$, the redundancy is typically less than 1.0 throughout loading and that the force threshold required for $R = 1$ leads to normalized values less than 1.0. The proportion of force chain particles in these networks at $f_c = 1$ and the isostatic threshold are above 99% throughout loading (not shown). Also, the

Journal: 10035 Article No.: 0250 MS Code: GRMA-D-10-00058.2 TYPESET DISK LE CP Disp.:2011/1/20 Pages: 7 Layout: Large

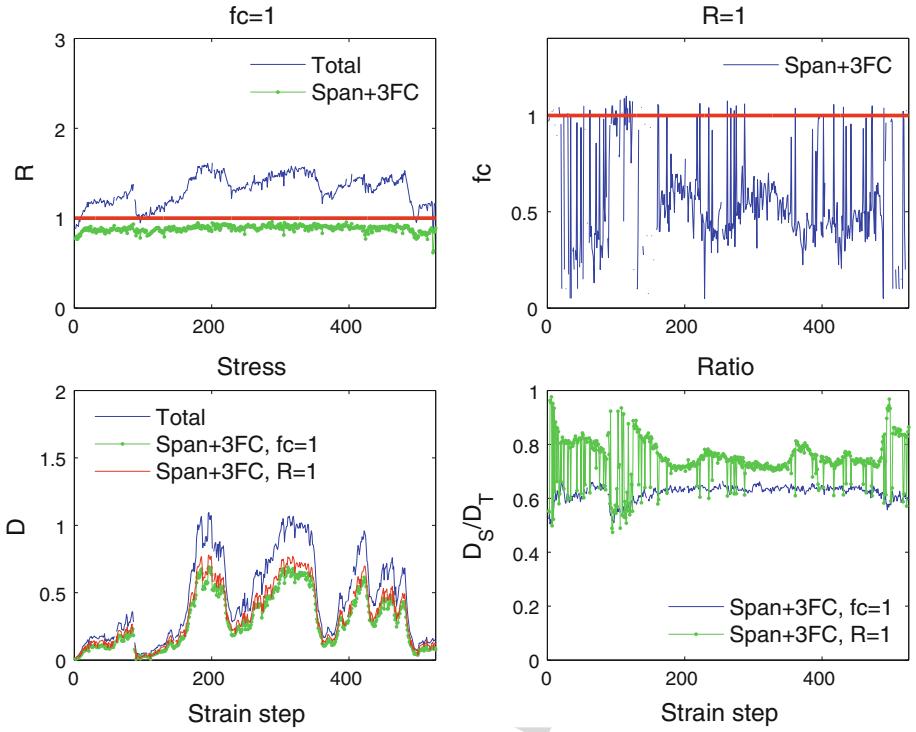

Fig. 4 Color online. Cyclic shear system—*Top left*: The redundancy of the networks at $f_c = 1$. *Top right*: the force threshold required such that the subnetwork (Span+3FC) is isostatic. *Bottom left*: the deviator stress $f_c = 1$ and $R = 1$. *Bottom right*: contribution to deviator stress of the subnetworks

deviator stresses of the subnetworks are highly correlated with, and are responsible for, a majority (typically >80%) of the total deviator stress. Figure 4 shows results for the experimental cyclic shear system. Due to the larger errors of determining contacts and contact forces, it is not always possible to find a rich enough starting network for all strain steps, and some are left blank. Furthermore, distinguishing stick, sliding, rolling and sliding and rolling modes of contact is slightly more involved than checking contact force and contact moment magnitudes. For surviving contacts between two disks across a strain step we track the position of the contact on each disk and the rotation of each disk. If either disk shows a non-zero rotation the contact is either a rolling or a sliding and rolling mode. If the change in position of the contact on either disk is only due to relative motion then the contact is rolling otherwise it is classed as sliding and rolling. If neither disk rotates but there is a change in position of contact then the mode of contact is sliding. A contact is classified as stick if none of the conditions for slide, roll, slide and roll is met [7]. The resulting subnetworks capture about 70% of the force chain particles for $f_c = 1$. This rises to an average of 92% for the isostatic subnetworks. The force threshold needed for the isostatic condition of $R = 1$, if it exists, can be very low, but can also be above the usual force threshold $f_c = 1$. Again throughout the loading, the deviator stress of the subnetworks are highly correlated with and can capture 60% (for $f_c = 1$) and 80% (for $R = 1$) of the macroscopic deviator stress.

4 Conclusion

We have presented a method for finding a percolating, strong subnetwork of contacts in a quasi-statically deforming granular material that contributes to the majority of the total deviator stress and is isostatic in the sense of R defined in (2) being equal to one. By a process of optimization that considers all contacts bearing a normal contact force magnitude above a given global force threshold, we find that the union of the 3-force-cycles and all the minimal spanning trees, optimized to include as many elastic contacts as possible, delivers such a subnetwork. If the threshold is set to the global average normal contact force, the resulting subnetwork will typically percolate across the system, include the majority of the force chain particles, and contribute to the majority of, as well as being highly correlated with, the total deviator stress. However, this subnetwork is just below the isostatic condition of $R = 1$. If the isostatic condition of $R = 1$ is used as a constraint, then the force threshold required to achieve this is less than $f_c = 1$ for the DEM but could be above $f_c = 1$ for stages of the deformation in the experimental system. The finding that granular materials are inherently bimodal, by which a percolating isostatic subnetwork of the material can be distinguished from the milieu of more lightly loaded particles, opens new avenues for future study. In particular, this has demonstrated how we can extract new insights from DEM and experiments to directly facilitate the continued development of structural mechanics models of force chain evolution such as that in [1], and of predictive continuum models such

uncorrected

Journal: 10035 Article No.: 0250 MS Code: GRMA-D-10-00058.2 TYPESET DISK LE CP Disp.:2011/1/20 Pages: 7 Layout: Large

as those proposed for isostatic systems in [24,25] and for the more general case in [29].

Acknowledgments We thank Fernando Alonso-Marroquin and our reviewers for their insightful comments and assistance which have significantly improved the paper. This study was supported by the US Army Research Office (W911NF-07-1-0131 for RPB, W911NF-07-1-0370 for AT) and the Australian Research Council (DP0986876 and DP0772409 for AT) and the US NSF (DMR0906908 for RPB).

References

1. Tordesillas, A., Muthuswamy, M.: J. Mech. Phys. Solids **57**, 706–727 (2009)
2. Vardoulakis, I.: Ingenieur-Archiv **59**, 106–113 (1989)
3. Drescher, A., de Josselin de Jong, G.: J. Mech. Phys. Solids **20**, 337–340 (1972)
4. Majmudar, T.S., Behringer, R.P.: Nature **435**, 1079–1082 (2005)
5. Zhang, J., Majmudar, T.S., Tordesillas, A., Behringer, R.P.: Granul Matter **12**, 159–172 (2010)
6. Tordesillas, A., Walker, D.M., Lin, Q.: Phys. Rev. E **81**, 011302 (2010)
7. Tordesillas, A., Lin, Q., Zhang, J., Behringer, R.P., Shi, J.Y.: J. Mech. Phys. Solids. (2010). doi:10.1016/j.jmps.2010.10.007
8. Tordesillas, A., Pucilowski, S., Walker, D.M., Peters, J., Hopkins, M.: Dynamics of Continuous, Discrete and Impulsive Systems-B: Applications & Algorithms, (in press)
9. Radjai, F., Jean, M., Moreau, J.-J., Roux, S.: Phil. Rev. Lett. **77**, 274–277 (1996)
10. Thornton, C., Antony, S.J.: Phil. Trans. R. Soc. Lond. A **356**, 2763–2782 (1998)
11. Thornton, C.: Geotechnique **50**, 43–53 (2000)
12. Antony, S.J., Kuhn, M.R.: Int. J. Solids Struct. **41**, 5863–5870 (2004)
13. Thornton, C., Zhang, L.: Geotechnique **60**, 333–341 (2010)
14. Antony, S.J.: Phil. Trans. R. Soc. A **365**, 2879–2891 (2007)
15. Bažant, Z.P., Cedolin, L.: Stability of Structures: Elastic, Inelastic, Fracture and Damage Theories. Oxford University Press, New York (2003)
16. Chakraborty, B., Behringer, R.P.: In: Encyclopedia of Complexity and System Science, **39**, 4997–5021. (2009)
17. van Hecke, M.: J. Phys. Condens. Matter **22**, 033101 (2010)
18. Liu, A.J., Nagel, S.R.: Annu. Rev. Condens. Matter Phys. **1**, 347–369 (2010)
19. Moukarzel, C.F.: Phys. Rev. Lett. **81**, 1634–1637 (1998)
20. Ellenbroek, W.G., Somfai, E., van Hecke, M., van Saarloos, W.: Phys. Rev. Lett. **97**, 258001 (2006)
21. Ellenbroek, W.G., van Hecke, M., van Saarloos, W.: Phys. Rev. E **80**, 061307 (2009)
22. Wyart, M., Silbert, L.E., Nagel, S.R., Witten, T.A.: Phys. Rev. E **72**, 051306 (2005)
23. Liu, A.J., Nagel, S.R.: Nature **396**, 21–22 (1998)
24. Blumenfeld, R.: Phys. Rev. Lett. **93**, 108301 (2004)
25. Blumenfeld, R.: New J. Phys. **9**, 160 (2007)
26. Walker, D.M., Tordesillas, A.: Int. J. Solids Struct. **47**, 624–639 (2010)
27. Tordesillas, A., Zhang, J., Behringer, R.P.: Geomech. Geoeng. **4**, 3–16 (2009)
28. Muthuswamy, M., Tordesillas, A.: J. Stat. Mech. Theory Exp. P09003 (2006)
29. Tordesillas, A., Muthuswamy, M.: Acta Geotechnica **3**, 225–240 (2009)

uncorrected proof

Journal: **10035** Article No.: **0250** MS Code: **GRMA-D-10-00058.2** ☐ TYPESET ☐ DISK ☐ LE ☐ CP Disp.:**2011/1/20** Pages: **7** Layout: **Large**